Energies **2014**, *7*, 3319-3338; doi:10.3390/en7053319

OPEN ACCESS

energies

ISSN 1996-1073

www.mdpi.com/journal/energies

Article

Design and Evaluation of a Photovoltaic/Thermal-Assisted Heat Pump Water Heating System

Huan-Liang Tsai

Department of Electrical Engineering, Da-Yeh University, No. 168, University Rd., Dacun, Chang-Hua 51591, Taiwan; E-Mail: michael@mail.dyu.edu.tw;
Tel.: +886-4-8511-888 (ext. 2204); Fax: +886-4-8511-245

Received: 13 March 2014; in revised form: 6 May 2014 / Accepted: 12 May 2014/ Published: 20 May 2014

Abstract: This paper presents the design, modelling and performance evaluation of a photovoltaic/thermal-assisted heat pump water heating (PVTA-HPWH) system. The cooling effect of a refrigerant simultaneously enhances the PVT efficiency and effectively improves the coefficient of performance (COP) of the HPWH system. The proposed model was built in the MATLAB/Simulink environment by considering the reciprocal energy exchange between a PVT evaporator and a HPWH system. In addition, the power consumption needs of the HPWH are provided by the PV electricity using a model-based control methodology. System performance is evaluated through a real field test. The results have demonstrated the power autarchy of the proposed PVTA-HPWH system with better PVT efficiency and COP. In addition, the good agreement between the model simulation and the experimental measurements demonstrate the proposed model with sufficient confidence.

Keywords: photovoltaic/thermal-assisted heat pump water heating (PVTA-HPWH); PVT evaporator; coefficient of performance (COP)

1. Introduction

With increasing attention being paid to the issue of global warming and the soaring cost of fuel, energy-efficient and environment-friendly heating and cooling applications ranging from domestic and commercial to industrial sectors are a promising development. Most residential water heating systems are equipped with conventional water heaters that utilize fossil fuels or electricity to generate heat and thus have a negative impact on the environment and offer low-efficiency energy conversion. With the characteristics of ubiquity, abundance, and sustainability, solar energy is currently considered the most

sustainable resource among the various renewable energy alternatives with the growing increase of environmental awareness. Photovoltaic/thermal (PVT) solar collectors that simultaneously produce electricity and heat are currently considered the most efficient devices to harness the available solar energy. Research and development on this topic has been promising during the last three decades. Some reviews on PVT collectors have recently been published [1–5]. On the other hand, heat pump (HP) systems can extract low-grade thermal energy from the environment and waste heat for use in water/space heating applications, therefore, they are currently considered as renewable energy sources in the EU [6] and UK [7]. In theory, the coefficient of performance (COP) of solar-assisted HP (SAHP) systems depends significantly on the temperature of the condenser and the temperature difference between the condenser and the evaporator [8]. Therefore, the waste heat recovery from solar cells for the evaporation of SAHP for water/space heating would mutually improve the PVT efficiency and the COP of SAHPs. Kern and Russel [9] revealed the high COP value of a PVT-SAHP system with the assistance of solar electricity and thermal energy. Ito and his team [10,11] have carried out continuous experimental studies on PVT-SAHP systems. Ji and his team have conducted some experimental evaluations of PVT-SAHP systems and validated them with a mathematical model [12–14]. Some improvements in the evaporator of PVT-SAHP systems based on theoretical simulation have been reported [15,16]. So far, the electrical characteristics of PV devices were not considered in the previous mathematical models of PVT-SAHP systems, when in fact, the thermodynamics of the PV module can directly integrate with the energy exchange of the PV output power [17]. It is found that the accuracy of the operating temperature estimation of the solar collector is the most important parameter in both PV electricity generation and reciprocal energy exchange. With the direct interaction of both PV electricity generation and the thermodynamics of the PVT collector, the concerted energy exchange between the PVT evaporator and HPWH system could be evaluated well and with better precision. Comparisons of the various literature approaches are listed in Table 1.

Table 1. Comparisons among PVT mathematical models.

Model types	Thermal characteristics	Electrical characteristics	References
Energy balance equation	$\rho_p C_p \delta_p \frac{\partial T_p}{\partial t} = [G(\alpha\tau)_p(1-\beta_c) + G(\alpha\tau)_c\beta_c - E - S] - h_a(T_p - T_a) - \varepsilon_p\sigma(T_p^4 - T_{sky}^4)$	$E = G\eta_{rc}[1-\beta(T_c - T_{rc})]\beta_c(\alpha\tau)_p$	Ji *et al.* [13]
Heat balance equation	$l_{pv}\rho_{pv}C_{pv}\frac{\partial T_{pv}}{\partial t} = G(\tau\beta)_{pv} - E + \alpha_{a-pv}(T_a - T_{pv}) + \alpha_{r,a-pv}(T_{sky} - T_{pv}) + \frac{T_c - T_{pv}}{R_{pv-c}}$	$E = G\tau_{eva}\eta_{ref}[1 - 0.0045(T_{pv} - 298.15)]$	Ji *et al.* [14]
Steady-state energy transfer equation	$l_{pv}\rho_{pv}C_{pv}\frac{\partial T_{pv}}{\partial t} = G(\tau\beta)_{pv} - E + \alpha_{a-pv}(T_a - T_{pv}) + \alpha_{r,a-pv}(T_{sky} - T_{pv}) + \frac{T_c - T_{pv}}{R_{pv-c}}$	$N_{pv} = I\tau_{pv}\eta_0[1 - C_T(t_p - 25)]A_{pv}$	Xu *et al.* [15]
Quasi-steady state energy balance equation	$Q_t = Q_{abs} - Q_l - Q_e = Q_r$	$Q_e = IA_{g,eff}\eta_{rc}[1 - \beta_p(t_{abs} - t_{rc})]$	Zhao *et al.* [16]
Thermodynamics equation	$m_{PVT}C_{PVT}\frac{dT_{PVT}}{dt} = Q_{Soalr} - Q_{Rad} - Q_{Conv} - P_{PV} - Q_{RF}$	$P_{PV} = N_p I_{PH} V - N_p I_S \left\{\exp\left[\frac{q}{kT_{PVT}A}\left(\frac{V}{N_S} + \frac{IR_S}{N_P}\right)\right] - 1\right\} V - \frac{1}{R_{SH}}\left(\frac{N_p V}{N_S} + IR_S\right)V$	Proposed model

Refrigerant-based PVT devices feature the best conversion efficiency of solar energy compared to air- or water-based PVT technologies. The PVT evaporator has advantages such as less area, higher performance, and cogeneration of solar electricity and thermal heat. They have the potential to activate and promote the Million Rooftop PVs project in Taiwan [18] as a suitable solution to the problem of limited residential space, therefore, a prototype of a PVT-assisted HPWH (PVTA-HPWH) system was implemented and studied. First, a rooftop PVT module is developed as a solar collector/evaporator and the PVT array is integrated with a HPWH system for solar assisted HPWH applications. Then the mathematical model for the dynamics of PVTA-HPWH system, including both electrical characteristics and thermodynamics of the PVT evaporator and HPWH system, and their energy exchange interaction were built using Simulink software. Having both a derivation of a mathematical model and after building a simulation model, the control system of a HPWH system is designed using model-based methodology subjected to optimal performance considerations. The system performance isfinally evaluated through the field test of a prototype PVTA-HPWH system.

2. System Description

The utility model patent of the novel PVTA-HPWH system was issued 21 June 2013 in Taiwan [19]. A rooftop PVT evaporator integrated with a commercial HPWH system was implemented for evaluating the performance of the PVT device and the COP of the HPWH system.

2.1. PVT Evaporator/Collector

A pre-coated steel sheet is folded using a CNC folder in the form of a troughed roof profile. As depicted in Figure 1, a rough PVT evaporator prototype with a rated power of 200 Wp was developed as a supporting structure, with multi-port cooper tubes adhered to the rear as thermal absorber, and polystyrene (PS) foam laid beneath as insulator.

Figure 1. PVT constituent layer: (**a**) Cross-sectional view; (**b**) Top view.

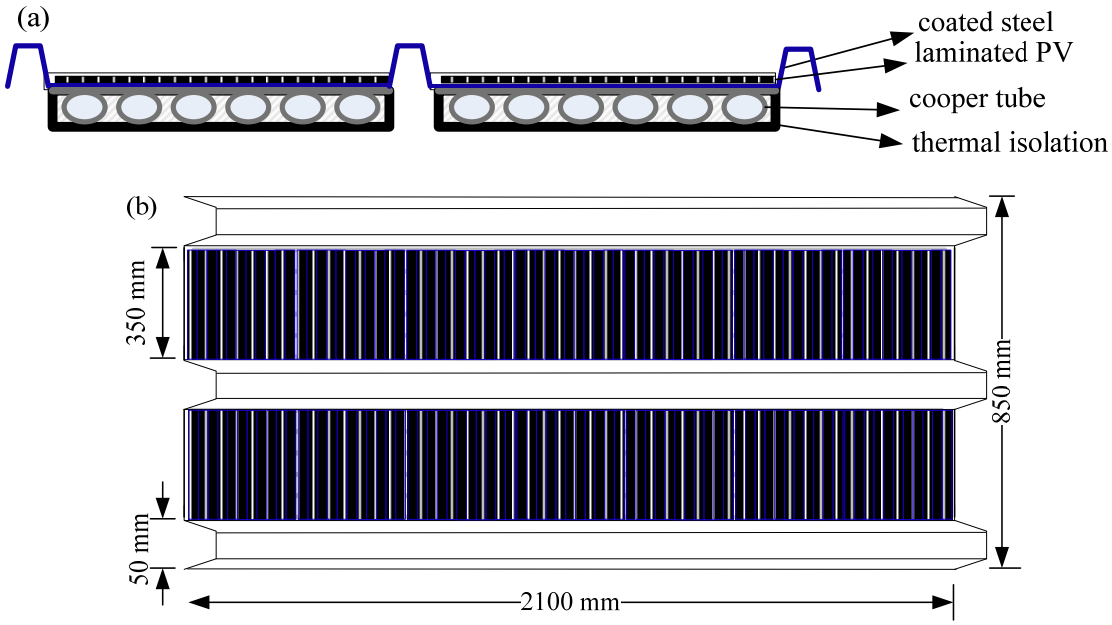

Forty-eight 6" 4.186 Wp polycrystalline silicon solar cells (Solartech Energy Corp., Hukou, Hsinchu, Taiwan) were arranged in two rows of twenty-four solar cells in series. The solar cells were sandwiched between ETFT and PET that were directly laminated in a steel coating like a PV module. A PT1000 (J-type thermocouple) sensor was laminated between the solar cells and steel sheet in the PV module encapsulation process. Based on the electrical characteristics of the solar cells under the standard test conditions (STC), *i.e.*, cell temperature of 25 °C and solar irradiance of 1 kW/m^2, the electrical characteristics can be estimated and are depicted in Figure 2. The associated electrical parameters are listed in Table 2, in which the temperature coefficients K_I and K_V are the rate of change (derivative) with respect to temperature of the short-circuit current I_{SC} and open-circuit voltage V_{OC}. The PVT evaporator/collector with R134a refrigerant fluid is the solar electricity converter and thermal energy collector.

Figure 2. $I-V$ and $P-V$ output characteristics of PVT module and notable points.

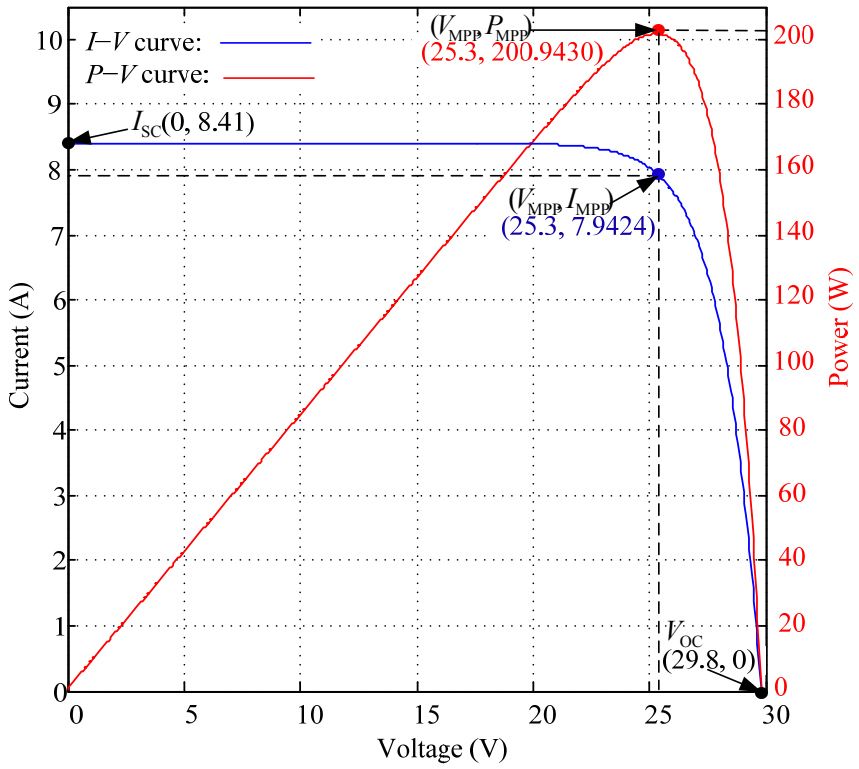

Table 2. PVT Specifications (1 kW/m^2, 25 °C).

Characteristics	Specifications
Maximum power rating (P_{MPP})	200.9 W
Rated voltage (V_{MPP})	25.3 V
Rated current (I_{MPP})	7.94 A
Short circuit current (I_{SC})	8.41 A
Open circuit voltage (V_{OC})	29.8 V
Temperature coefficient of open-circuit voltage (K_V)	−95 mV/°C
Temperature coefficient of short-circuit current (K_I)	6.7 mA/°C
Nominal operating cell temperature (NOCT)	46 °C

2.2. PVTA-HPWH System

The PVT evaporator is connected with a 1 kW HPWH system that is commercially available and works with environmentally friendly R134a refrigerant. The outside view of the PVT evaporator and a schematic diagram of the prototype system with rated power of 1 kWp is shown in Figure 3.

Figure 3. PVTA-HPWH system: (**a**) photo of PVT evaporator array; (**b**) PVTA-HPWH test rig.

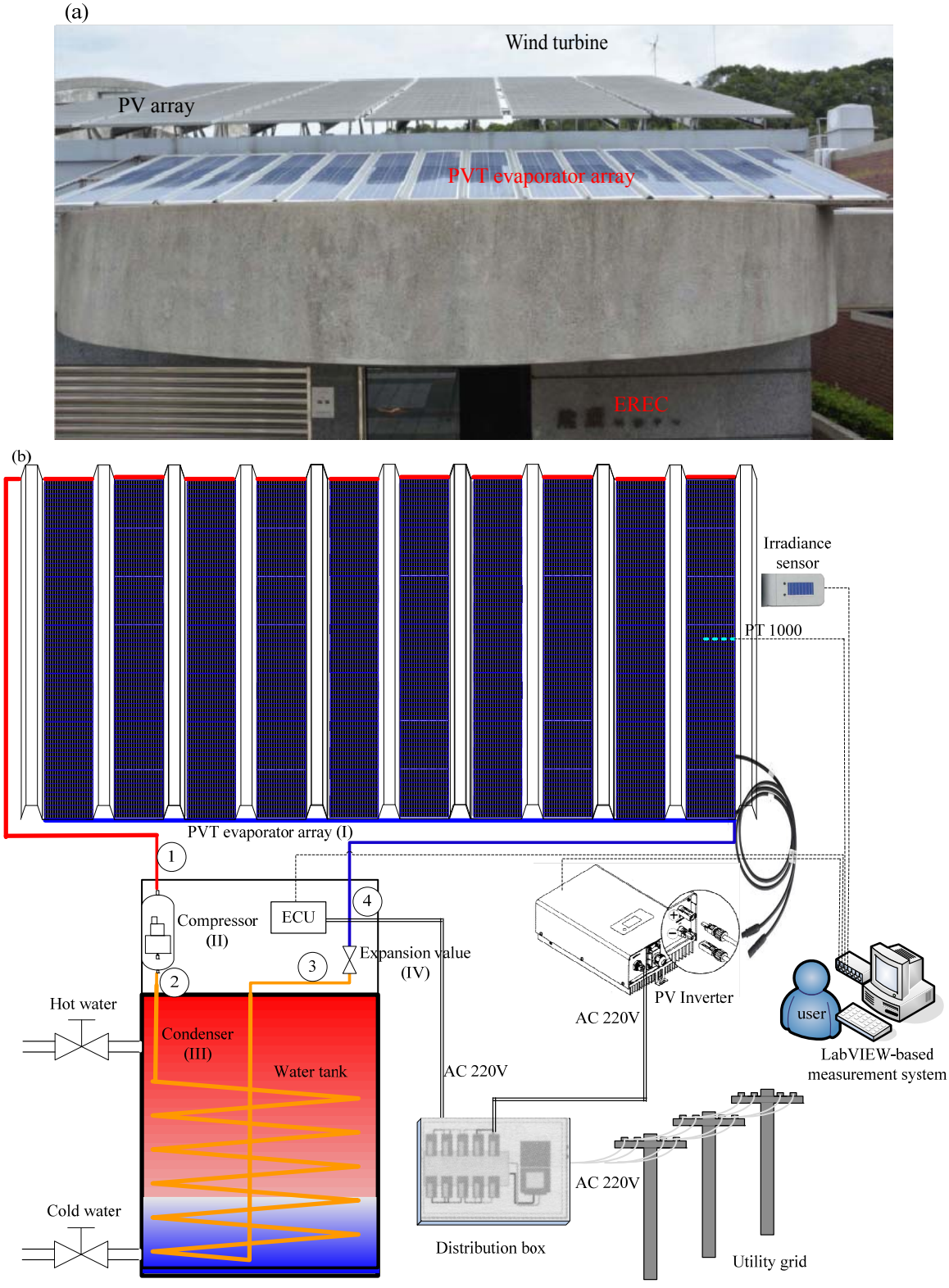

The PVTA-HPWH consists of a PVT evaporator array (I), a variable-frequency compressor (II, 2P19S3R236A-1A, Panasonic, Secaucus, NJ, USA), a condenser (III) immersed in a water tank, and an electronic expansion value (IV, AKVA, Danfoss, New Taipei City, Taiwan). The thermodynamics data of the refrigerant R134a, which depend on the working pressure and temperature of the PVT evaporator at different working points, are calculated by the Peace software [20] and are listed in Table 3.

Table 3. Thermodynamics data of the R134a refrigerant at different points of the PVTA-HPWH system.

Point	Phase	Pressure (bar)	Temperature (°C)	Enthalpy (kJ/kg)
1	Vapor	4.146	25	418.1
2	Vapor	14.915	65	437.5
3	Liquid	16.822	60	287.4
4	Liquid/ Vapor (x = 0.3876)	4.146	10	287.5

Figure 4 depicts the corresponding pressure-enthalpy chart. The PVT evaporator array consists of five rooftop PVT modules that are connected electrically in series and their refrigerant tubes are connected in parallel in the form of an external manifold. While flowing through the PVT evaporator (I), the refrigerant is directly vaporized.

Figure 4. Pressure-enthalpy diagram of the PVTA-HPWH cycle.

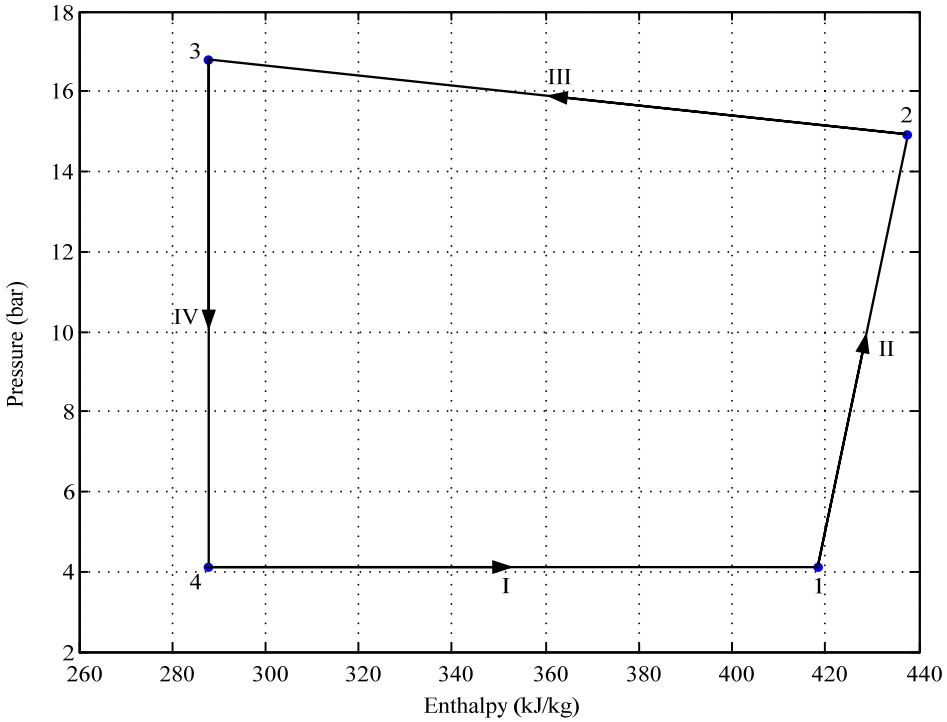

The direct expansion (DX) of refrigerant is expressed as the 4 → 1 process. In addition, the PVT evaporator generates solar electricity that can provide for the consumption of the compressor, electric control unit (ECU) and instruments. The vaporized refrigerant is compressed in the compressor (II) as the 1 → 2 process and is further upgraded to an appropriate temperature for heating purposes. The high-grade heat is then delivered into the condenser (III) to reject the useful heat into water (2 → 3

process). After being condensed, the high-pressure refrigerant is sent to an electric-controlled expansion value (IV) where undergoes a throttling process and collects as low-pressure liquid. This is expressed as the 3 → 4 process. Lowering the working temperature of the PVT evaporator not only increases PV efficiency due to the lower cell temperature but also enhances high the thermal efficiency with the heat recovery of ambient air. The rated power of PV electricity is designed enough to address the power consumption of the HPWH system.

3. System Modelling

There are three energy transfer mechanisms involved in the PVT evaporator: the PV effect that converts solar energy into solar electricity, thermal transportation that conveys solar radiation into the PVT collector and interchanges with the ambient environment, and heat recovery that evaporates the refrigerant within the coil for the evaporation of HPWH system. Its dynamic equation is given by:

$$m_{\mathrm{PVT}} C_{\mathrm{PVT}} \dot{T}_{\mathrm{PVT}} = Q_{\mathrm{Solar}} - Q_{\mathrm{Rad}} - Q_{\mathrm{Conv}} - P_{\mathrm{PVT}} - Q_{\mathrm{RF}} \tag{1}$$

where, m_{PVT}, C_{PVT}, and T_{PVT} are the mass, heat capacity, and temperature of PVT modules; Q_{Solar} is the net solar radiation reaching the PVT's front surface; Q_{Rad} is the long-wave radiation heat exchange in the background equivalent environment; Q_{Conv} is the convective heat exchange between BIPVT front surface and ambient air; P_{PVT} the PVT output power; and Q_{RF} is the removed heat through refrigerant. The associate thermal coefficients can be found in Duffie and Beckon [21]. The effective irradiation on PVT module is given by:

$$Q_{\mathrm{Solar}} = \alpha G A_{\mathrm{PVT}} \tag{2}$$

where, α is the PVT absorptivity; G is the incoming solar irradiance; and A_{PVT} is the PVT surface area. The long-wave radiation heat exchange in the equivalent background environment (sky, ground, and surroundings) is given by:

$$Q_{\mathrm{Rad}} = \sigma \varepsilon_{\mathrm{PVT}} \left(T_{\mathrm{PVT}}^4 - T_{\mathrm{Amb}}^4 \right) A_{\mathrm{PVT}} \tag{3}$$

where, σ is the Stefan-Boltzmann's constant; $\varepsilon_{\mathrm{PVT}}$ is the PVT emissivity. The forced convection from the front surface is considered and is given by:

$$Q_{\mathrm{Conv}} = h_{\mathrm{Conv}} \left(T_{\mathrm{PVT}} - T_{\mathrm{Amb}} \right) A_{\mathrm{PVT}} \tag{4}$$

where, h_{Conv} is the forced convection coefficient considering the effect of thermal radiation that can be approximated as a function of wind speed, which is given by:

$$h_{\mathrm{Conv}} = 2.8 + 3 v_{\mathrm{Wind}} \tag{5}$$

where, v_{Wind} is the wind speed.

Solar cells are arranged in the PVT evaporator with a series-parallel configuration for electricity generation applications. PV devices naturally exhibit nonlinear $I-V$ and $P-V$ characteristics that vary with radiant intensity and cell temperature. The $I-V$ output characteristic of the PVT evaporator with solar cells in N_{P} parallel and N_{S} series is given by:

$$I = N_{\mathrm{P}} I_{\mathrm{PH}} - N_{\mathrm{P}} I_{\mathrm{S}} \left\{ \exp\left[\frac{q}{kT_{\mathrm{PVT}} A} \left(\frac{V}{N_{\mathrm{S}}} + \frac{IR_{\mathrm{S}}}{N_{\mathrm{P}}} \right) \right] - 1 \right\} - \frac{1}{R_{\mathrm{SH}}} \left(\frac{N_{\mathrm{P}} V}{N_{\mathrm{S}}} + IR_{\mathrm{S}} \right) \tag{6}$$

where, I_{PH} is the photocurrent; I_{S} is the cell saturation of dark current; q is the charge of an electron; k is the Boltzmann's constant; A is the ideal factor that depends on PV technology; R_{SH} and R_{S} are the resistance of the shunt and series resistors. The photovoltaic current mainly depends on the solar irradiance and cell's working temperature as follows:

$$I_{\mathrm{PH}} = \left[I_{\mathrm{SC}}^{\mathrm{STC}} + K_{\mathrm{I}} \left(T_{\mathrm{PVT}} - T_{\mathrm{PVT}}^{\mathrm{STC}} \right) \right] \frac{G}{G^{\mathrm{STC}}} \tag{7}$$

where, $I_{\mathrm{SC}}^{\mathrm{STC}}$ is the short-circuit current of PV device at STC; K_{I} is the temperature coefficient of cell's short-circuit current. In addition, the cell's saturation current varies with the cell temperature, which is described as:

$$I_{\mathrm{S}} = I_{\mathrm{RS}} \left(\frac{T_{\mathrm{PVT}}}{T_{\mathrm{PVT}}^{\mathrm{STC}}} \right)^3 \exp\left[\frac{qE_{\mathrm{BG}}}{kA} \left(\frac{1}{T_{\mathrm{PVT}}^{\mathrm{STC}}} - \frac{1}{T_{\mathrm{PVT}}} \right) \right] \tag{8}$$

where, I_{RS} is the cell's reverse saturation current; E_{BG} is the band-gap energy of the semiconductor used in the cell. With an operating voltage, the BIPVT output power is:

$$P_{\mathrm{PVT}} = IV \tag{9}$$

In the evaporation procedure, the low-grade heat of solar collector is obtained as:

$$Q_{\mathrm{RF}} = \dot{m}_{\mathrm{RF}} \left(H_1 - H_4 \right) \tag{10}$$

where, H_i is the enthalpy of refrigerant in the i state, which is related to the working pressure and temperature of refrigerant. In PVT evaporator, the average specific enthalpy of the refrigerant is determined by the vapor quality and the specific enthalpy at the saturated and vapor states that is calculated by:

$$H_4 = xH_{vapor} + (1-x)H_{liquid} \tag{11}$$

where, x is the vapor quality that carries a value of $0 < x < 1$ in the two-phase flow region. The electric power consumption of compressor P_{CP} and the heat transfer of a condenser Q_{CD} have been derived in [13,14,18,19].

Based on the mathematical formulation of PVTA-HPWH system, a simulation model is built in the MATLAB/Simulink environment. The proposed PVTA-HPWH model having direct interaction of PV electricity with the thermodynamics is built. First, the overall PVTA-HPWH system is decomposed into the PVT evaporator and HPWT subsystems that are created as subsystem blocks. The PVTA-HPWH block is masked with a user-friendly icon as shown in Figure 5a. Then the block diagram of the subsystem is built to mathematically characterize both the thermodynamics and electricity of the PVT evaporator and HPWH system as shown in Figure 5b.

Figure 5. PVTA-HPWT Simulink model: (**a**) masked icon; (**b**) subsystem implementation.

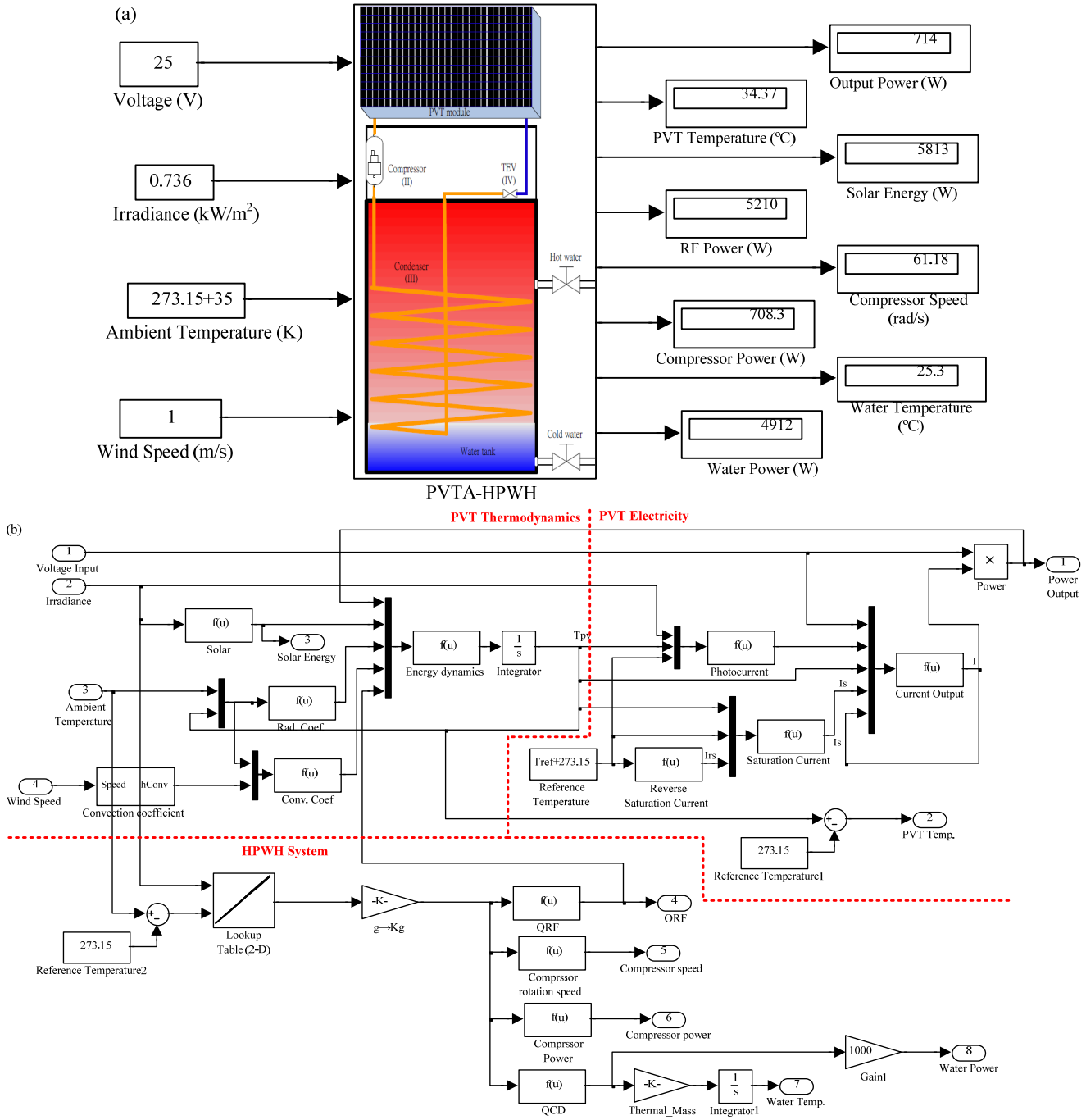

In the subsystem, the thermal dynamical equation and its associate solar radiation, long-wavelength radiation, forced convection of wind and convection of refrigerant are implemented using the built-in Fcn blocks in Simulink. The PV electrical characteristics such as $I-V$ characteristic equation, photovoltaic current, cell's saturation current and reverse saturation current are implemented in the same way.

Model-based methodology is one kind of optimal control design technology. Based on the mathematical/simulation model, the predicted control system is designed subject to optimal performance considerations. Having a well-validated PVTA-HPWH model, the control gain can be found with the increase in solar irradiance from 0 to 1000 W/m^2 at the interval of 200 W/m^2, and the

ambient temperature from 20 °C to 40 °C at a 5 °C step. The control gains for the mass flow rate of refrigerant are listed in Table 4 and are built in Figure 4b. The control gain is a function of solar irradiance and PVT temperature.

Table 4. Control gains for mass flow rate of refrigerant (unit: g).

Irradiance(W/m^2)	Temperature (°C)				
	20	**25**	**30**	**35**	**40**
0	0	0	0	0	0
200	10.38	10.65	10.97	11.34	11.79
400	20.98	21.26	21.58	21.96	22.41
600	31.59	31.87	32.30	32.58	33.04
800	42.20	42.48	42.81	43.20	43.66
1000	52.80	53.09	53.43	53.82	54.28

4. Experimental Evaluation

4.1. Experimental Rig

As illustrated in Figure 3b, the experiment setup consists of the PVT array, a commercial PV inverter with a rated power of 1.5 kW, a HPWH system with a rated power of 1 kWp and water tank capacity of 200 L, and some instruments. The PVT array was mounted on rooftop and placed in a south-facing position with an inclination angle of 23.5°. A pyrameter (Fronious Mono-Crystalline Si-Sensor, Tullamarine, Austria) was mounted at the same inclination of the PVT device to measure incident solar irradiation on the PVT plate. A temperature sensor (PT1000, J-type thermocouple) sensor laminated between the solar cell and steel sheet in the encapsulation process of the PV module was used to measured the lump PVT temperature parameter. The PV inverter has a good MPP tracker and PV electricity is fed into the utility grid through a distribution box. Its SolarPower software provides information about working voltage, output current and PV electricity power. Each sensor has its own relative error as listed in Table 5. The electric control unit (ECU) in the HPWH system is designed to monitor and control the system operation according to its thermodynamic data, In addition, the ECU controls the input current and power consumption for autonomous operation based on the energy balance equation. A LabVIEW-based automated measurement system has been designed to automatically visualize the electric and thermal data of the PVT, the parameters of HPWH system, and surrounding conditions such as solar irradiance, ambient temperature, and wind speed. The sampling period is set at an interval of 1-minute. The overall experiment rig was set up in the Energy Research and Development Center (ERDC) of Da-Yeh University in Taiwan.

Table 5. Relative errors of the sensors.

Sensor	Accuracy	Operating temperature
Irradiance	±5%	−40 °C–80 °C
Temperature	±0.8 °C	−40 °C–100 °C
Wind speed	±5%	−20 °C–65 °C
Electricity	±5%	−20 °C–50 °C

4.2. Experimental Results

A one-hour measurement of the experiment rig was conducted from 12:00 to 13:00 for each day during June 2013. All observations of the physical parameters were automatically recorded at 1-min intervals. The results for two typical days with blue-sky and mostly sunny weather conditions are presented. The solar irradiance and ambient temperature for a typical sunny day (18 June 2013) are depicted in Figure 6a,b.

Figure 6. Measured and simulated data on a typical sunny day (18 June 2013): (**a**) Solar irradiance and radiation; (**b**) Ambient and PVT temperatures; (**c**) Measured and simulated PV output current and its power; (**d**) Compressor power and measured PV output power; (**e**) Measured and simulated water temperature and storage energy.

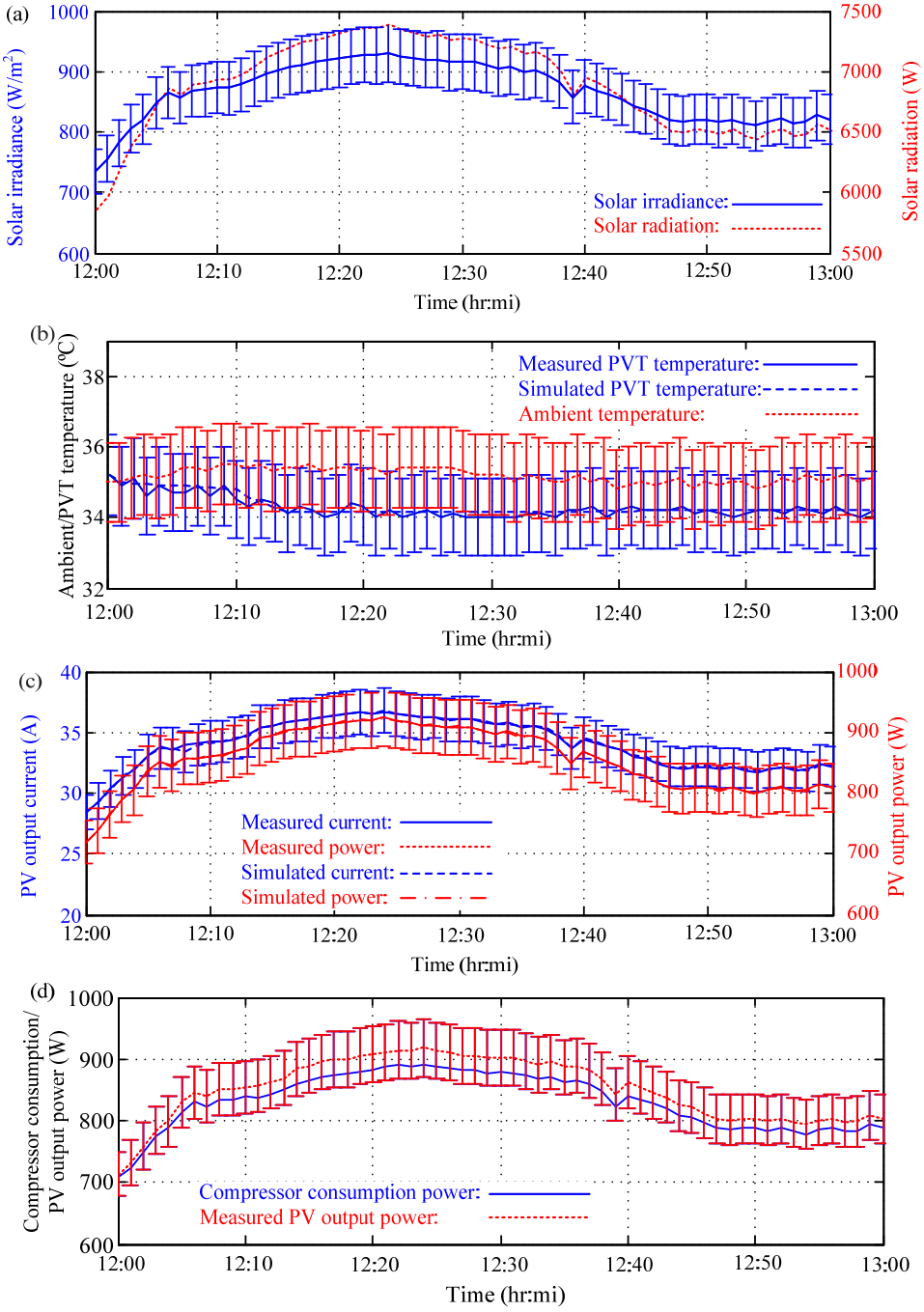

Figure 6. *Cont.*

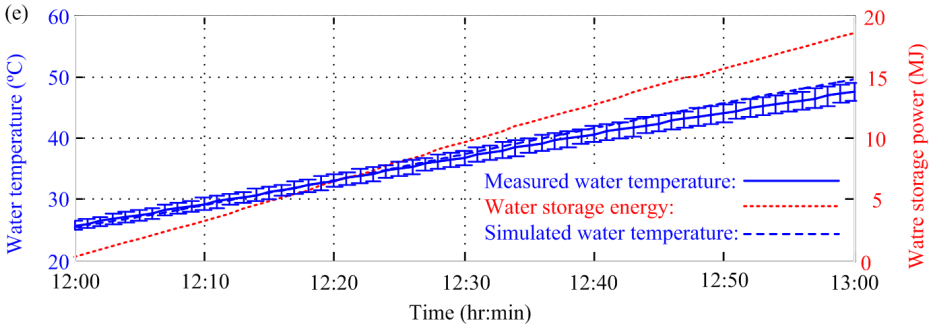

For easy comparison, the measured and simulated operating temperatures of PVT module are shown in Figure 6b. The results reveal that temperature difference is less than ±0.35 °C and its root mean square (RMS) value is 0.1339 °C. Considering the ±0.8 °C accuracy (in the range of −40 °C to 100 °C) of the PT1000 sensor, the prediction accuracy of PVT temperature is ±1.15 °C. Therefore, the simulated and measured results of the output current and power the PVT collector are almost close to each other as represented in Figure 6c. The maximal difference between the measured and simulated output current is 0.3 A and the RMS of difference is 0.1076 A. In addition, the maximal difference between the measured and simulated output power is 1.2 W and the associated RMS is 0.6305 W. Figure 6d shows the power consumption of the compressor of HPWH system and the result reveals PV electricity is enough to afford the compressor operation. The water temperature and energy in the water tank are depicted in Figure 6e. The results of the difference and RMS analyses are listed in Table 6.

Table 6. Difference analysis for both a typical sunny day (18 June 2013) and a mostly sunny day (12 June 2013).

Weather type	Items	PVT temperature	Output current	Output current
Typical sunny day	difference	±0.35 °C	0–0.3 A	0–1.2 W
	RMS	0.1339 °C	0.1076 A	0.6305 W
Mostly sunshine day	difference	±0.4 °C	0–0.3 A	0–1.5 W
	RMS	0.1744 °C	0.1636 A	0.9277 W

For a mostly sunny day (12 June 2013), the solar irradiance and ambient temperature are depicted in Figure 7a,b. The average of wind speed is 3 m/s for the duration of the experiment. There are fluctuations in solar irradiance and ambient temperature near 12:10. Both measured and simulated operating temperatures of PVT module are shown in Figure 7b and the maximal difference is less than ±0.4 °C that occurs near the falling and rising duration of the climate fluctuation. The associated RMS of the temperature difference is 0.1744 °C. Both simulated and measured output current and power the PVT collector are depicted in Figure 7c. The maximal difference between the measured and simulated output current is also 0.3 A and the RMS of difference is 0.1636 A. In addition, the maximal difference between the measured and simulated output power is 1.5 W and the associated RMS is 0.9277 W. The power consumption of the compressor of HPWH system is also lower than the PV electricity as shown in Figure 7d. The water temperature and energy in the water tank are depicted in Figure 7e. The difference and RMS analyses for such a mostly sunshine day are also listed in Table 6.

Figure 7. Measured and simulated data on a mostly sunny day (12 June 2013): (**a**) Solar irradiance and radiation; (**b**) Ambient and PVT temperatures; (**c**) Measured and simulated PV output current and its power; (**d**) Compressor power and measured PV output power; (**e**) Measured and simulated water temperature and tank storage energy.

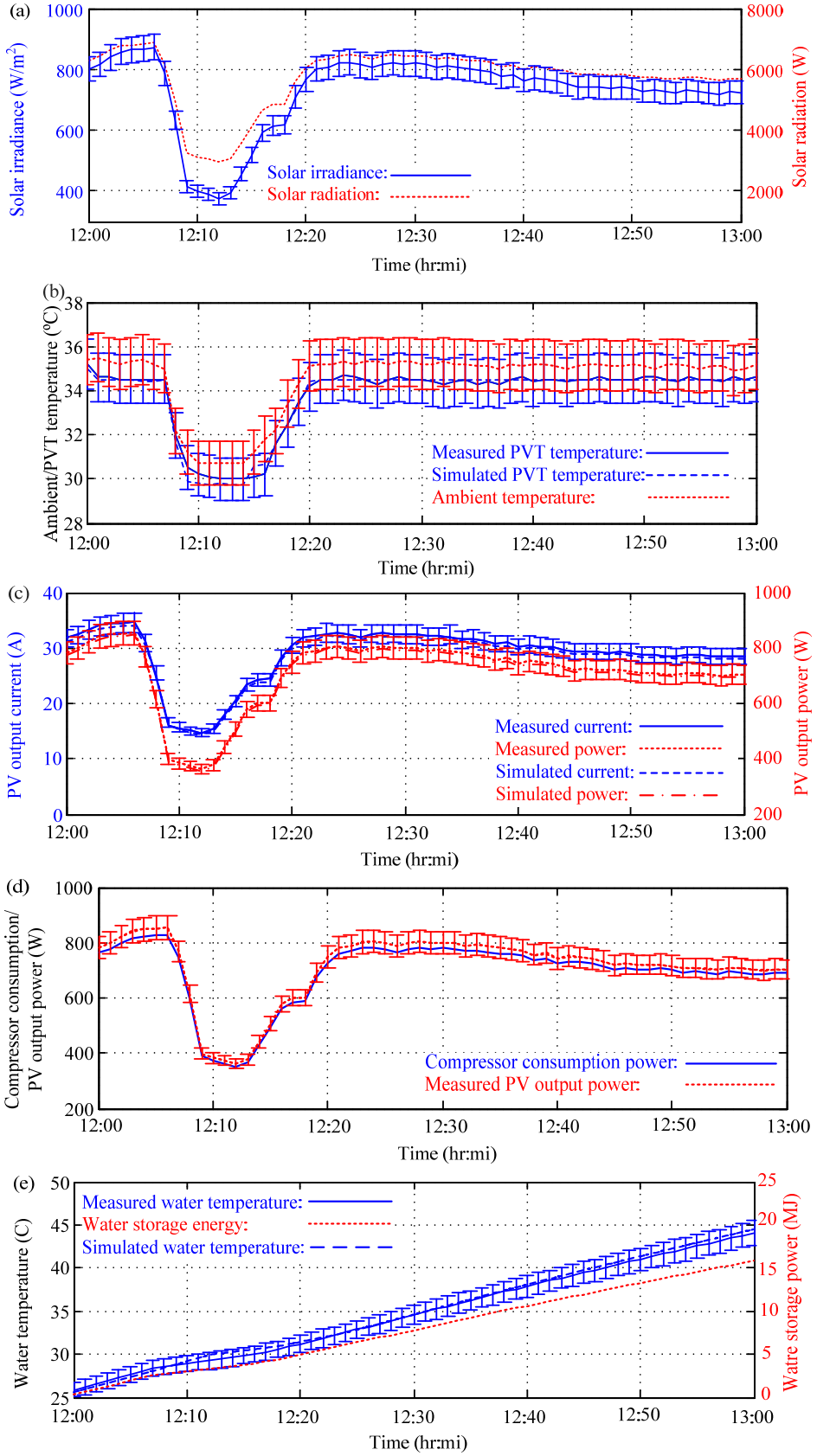

From above analysis, it is seen that the proposed PVTA-HPWH model has a sufficient degree of accuracy under real sunny and mostly sunshine weather conditions. Even in face of the fluctuations of weather conditions, the model confidence is enough to predict the operation situations of overall PVTA-HPWH system. It should be noted that the proposed model slightly underestimates the output current and power posed to the overestimation of PVT temperature.

4.3. Performance Evaluation

From the viewpoint of energy utilization, the energy efficiency of the PVTA-HPWH is the summation of the efficiency of PV electricity generation and the thermal efficiency of water heating:

$$\eta_{\mathrm{PV}} = \frac{P_{\mathrm{PVT}}}{Q_{\mathrm{Solar}}} \tag{12}$$

$$\eta_{\mathrm{TH}} = \frac{Q_{\mathrm{RF}}}{Q_{\mathrm{Solar}}} \tag{13}$$

and

$$\eta_{\mathrm{PVT}} = \eta_{\mathrm{PV}} + \eta_{\mathrm{TH}} \tag{14}$$

On the other hand, the comprehensive coefficient of thermal-to-electrical performance (COP) for the PVTA-HPWH system is defined as [3]:

$$\mathrm{COP} = \frac{Q_{\mathrm{CD}}}{P_{\mathrm{CP}}} \tag{15}$$

where, P_{CP} is the power consumption of compressor and Q_{CD} is the heat transfer of a condenser.

Figure 8 demonstrates the corresponding efficiencies of the PVT device, including electrical, thermal, and the total efficiencies, for the sunny day (18 June 2013). The associated COP of the overall PVTA-HPWH system is also represented in Figure 8.

The solar electricity efficiency is in the range of 12.2%–12.5% with an average of 12.43% and the solar thermal efficiency is in the range of 73.70%–74.00% with an average of 73.80%. The total efficiency of the PVT device is in the range of 86.18%–86.27% with an average of 86.23%. It should be noted that some thermal energy is recovered from the surroundings because the PVT temperature is lower than the ambient one. On the other hand, the COP of the integrated PVTA-HPWH system is in the range of 7.01–7.10 with an average of 7.09. With the temperature upgrade of PVT evaporator, the power consumption of compressor is relieved. In addition, the PV efficiency is enhanced due to the cooling effect of refrigerant. The mean results of the efficiency of PVT evaporators and the COP of overall system are listed in Table 7.

Figure 8. Performance analysis of PVTA-HPWH system on a typical sunny day (18 June 2013): (**a**) PV and thermal efficiency; (**b**) COP.

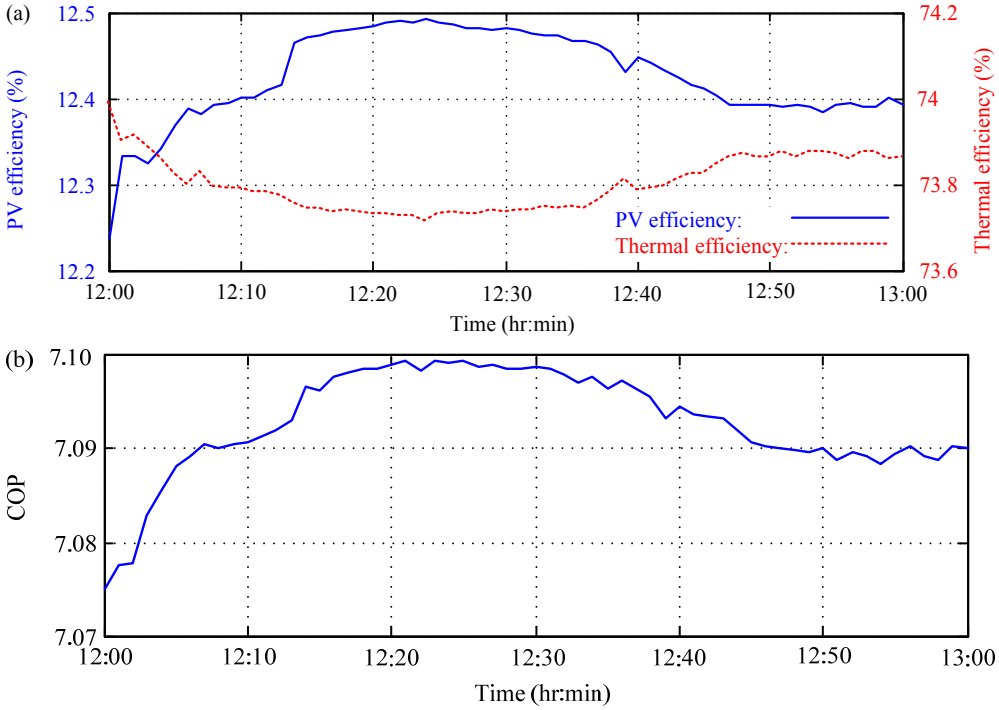

Table 7. Mean analysis of efficiency and performance for both a typical sunny day (18 June 2013) and a mostly sunny day (12 June 2013).

	PV efficiency	Thermal efficiency	Total efficiency	COP
Typical blue-sky day (18 June 2013)	12.43%	73.80%	86.23%	7.09
Mostly sunshine day (12 June 2013)	12.37%	73.90	86.29	7.09

For a mostly sunny day (12 June 2013), the electrical, thermal, and the total efficiencies of PVT device as well as the associated COP of the overall PVTA-HPWH system are depicted in Figure 9.

The solar electricity efficiency is in the range of 12.2%–12.5% with an average of 12.37% and the solar thermal efficiency is in the range of 73.70%–74.00% with an average of 73.90%. The total efficiency of the PVT device is in the range of 86.0%–86.5% with an average of 86.29%. On the other hand, the COP of the integrated PVTA-HPWH system is in the range of 7.07–7.10 with an average of 7.09. It should be pointed out that the fluctuation of solar irradiance does have a negative effect on the efficiency of the PVT device and the COP of PVTA-HPWH system. The mean results of both PVT efficiency and overall COP are also listed in Table 7.

Figure 9. Performance analysis of PVTA-HPWH system on a mostly sunny day (12 June 2013): (**a**) PV and thermal efficiency; (**b**) COP.

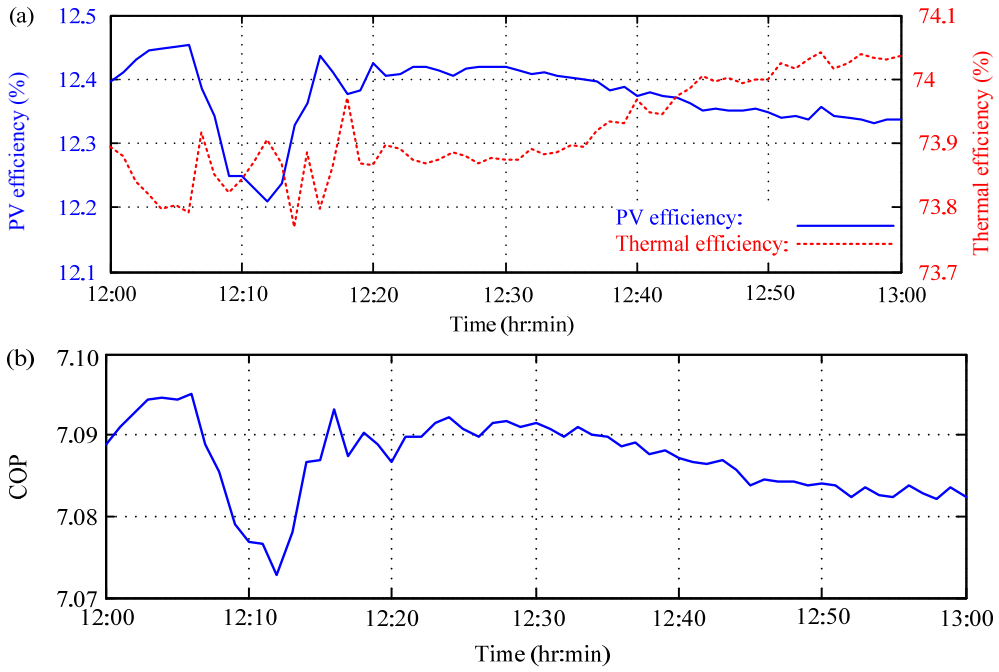

5. Conclusions

In this paper a self-sufficient design for a PVTA-HPWT system was represented and validated with the proposed model and an experimental test rig under real weather conditions during June 2013. The swift changes of weather conditions have little negative effect on the performance of the PVTA-HPWH system. It does not affect the normal operation of the overall system from the viewpoint of dynamics. The solar electricity of rooftop PVT devices can provide the power consumption needs of compressor in the HPWH system. The following conclusions can be drawn:

(1) With a well-validated PVTA-HPWH model and the mass flow rate of refrigerant from the model-based prediction control, the results show that the proposed PVTA-HPWT model has sufficient confidence even in face of sunshine fluctuations. Swift changes of weather conditions have a small negative effect on the performance of the PVTA-HPWH system, but it does not affect the normal operation of the overall system from the viewpoint of dynamics;

(2) With the self-sufficient operation design for the PVTA-HPWT system, the solar electricity of PVT array is able to provide the power needed by the compressor in the HPWH system based on the model-based prediction control methodology;

(3) With the cooling effect of refrigerant on PVT devices, the PV efficiency can be improved. In addition, low-temperature refrigerant can directly extract ambient heat through the PVT array. This obviously enhances the thermal efficiency of PVT devices. The total PVT efficiency and the COP of the PVTA-HPWH system reach up to 86% and 7.09, respectively.

Acknowledgments

The author gratefully acknowledges the financial support by the projects NSC 101-2212-E-212-016 and NSC 102-2221-E-212-017 from Ministry of Science and Technology of the Republic of China.

Nomenclature

A	ideal factor
A_{PVT}	PVT area (m^2)
C_{PVT}	PVT heat capacity $[\mathrm{J/(kg \cdot K)}]$
E_{BG}	band gap of cell (in eV).
G	solar irradiance ($\mathrm{kW/m^2}$)
G^{STC}	standard test irradiance of 1 $\mathrm{kW/m^2}$
h_{Conv}	convection coefficient $[\mathrm{W/(m^2 \cdot K)}]$
h_{PVT2RF}	heat transfer coefficient $[\mathrm{W/(m^2 \cdot K)}]$
H_i	enthalpy of refrigerant in *i* state (J/kg)
i	*i* state of HPWH operation
I_{MPP}	rated output current at MPP in ampere (A)
I_{PH}	photocurrent in ampere (A)
I_{RS}	reverse saturation current in ampere (A)
I_{S}	dark current in ampere (A)
$I_{\mathrm{SC}}^{\mathrm{STC}}$	PV short circuit current at STC in ampere (A)
k	Boltzmann's constant ($=1.38\times10^{-23}\mathrm{J/K}$)
K_{I}	short circuit current temperature coefficient ($\mathrm{A/^\circ C}$)
K_{V}	open circuit voltage temperature coefficient ($\mathrm{V/^\circ C}$)
m_{PVT}	PVT mass (kg)
N_{P} (N_{S})	parallel (series) number of cells
P_{MPP}	maximum power rating at MPP in watt (W)
P_{CP} (P_{PVT})	compressor (PVT) power in watt (W)
q	electron charge ($=1.6\times10^{-19}\mathrm{C}$)
Q_{Conv}	convective heat loss in watt (W)
Q_{Rad}	long-wave radiation heat exchange in watt (W)
Q_{RF}	heat removed by refrigerant in watt (W)
Q_{Solar}	solar irradiation in watt (W)
R_{S} (R_{SH})	series (shunt) resistance in ohm (Ω)
T_{Amb}	ambient temperature in Kelvin (K)
T_{PVT} ($T_{\mathrm{PVT}}^{\mathrm{STC}}$)	PVT cell temperature (at STC) in Kelvin (K)
v_{Wind}	wind speed (m/s)
V_{MPP}	rated operating voltage at MPP in voltage (V)

V_{OC}	open circuit voltage in voltage (V)
x	vapor quality

Greek Letters

α	PVT absorptivity
ε_{PVT}	PVT emissivity
η	efficiency
σ	Stefan-Boltzmann's constant

Abbreviations

Amb	ambient
BG	band gap
Conv	convection
CD	condenser
COP	coefficient of performance
CP	compressor
HPWH	heat pump water heating
MPP	maximum power point
OC	open circuit
P	parallel
PV	photovoltaic
PVT	PVT device
PVTA	PVT assisted
Rad	long-wave radiation
RF	refrigerant
RS	reverse saturation
S	series
SAHP	solar-assisted heat pump
Solar	Solar irradiance
SC	short circuit
SH	shunt
STC	standard test condition
TH	thermal

Conflicts of Interest

The author declares no conflict of interest.

References

1. Zondag, H.A. Flat-plat PV-thermal collector and system: A review. *Renew. Sustain. Energy Rev.* **2009**, *12*, 891–959.

2. Chow, T.T. A review on photovoltaic/thermal hybrid solar technology. *Appl. Energy* **2010**, *87*, 365–379.
3. Hasan, M.A.; Sumathy, K. Photovoltaic thermal module concepts and their performance analysis: A review. *Renew. Sustain. Energy Rev.* **2010**, *14*, 1845–1859.
4. Ibrahim, A.; Othman, M.Y.; Ruslan, M.H.; Mat, S.; Sopian, K. Recent advances on flat plat photovoltaic/thermal (PV/T) solar collectors. *Renew. Sustain. Energy Rev.* **2011**, *15*, 352–365.
5. Tyagi, V.V.; Kaushik, S.C.; Tyagi, S.K. Advancement in solar photovoltaic/thermal (PV/T) hybrid collector technology. *Renew. Sustain. Energy Rev.* **2012**, *16*, 1383–1398.
6. The European Parliament and The Council of the European Union, "Directive 2009/28/EC of the European Parliament and of the Council of 23 April 2009 on the promotion of the use of energy from renewable sources and amending and subsequently repealing Directives 2001/77/EC and 2003/30/EC," Official Journal of the European Union, May 2009, pp. L140/16–62. Available online: http://faolex.fao.org/docs/pdf/eur88009.pdf (accessed on 15 May 2014).
7. Barker, G. *Renewable Energy Incentive*; UK Department of Energy and Climate Change: London, UK, 2011.
8. Chwieduk, D.A. Solar-assisted heat pump. In *Comprehensive Renewable Energy*; Sayigh, A., Ed.; Elsevier Ltd.: Oxford, UK, 2012; Volume 3, pp. 495–528.
9. Kern, E.C., Jr.; Russel, M.C. Combined photovoltaic and thermal hybrid collector system. In Proceedings of the 13th IEEE Photovoltaic Specialists Conference, Washington, DC, USA, 5–8 June 1978; pp. 1153–1157.
10. Ito, S.; Miura, N.; Wang, J.Q. Heat pump using a solar collector with photovoltaic modules on the surface. *J. Sol. Energy Eng.* **1997**, *119*, 147–151.
11. Ito, S.; Miura, N.; Takano, Y. Studies of heat pump using direct expansion type solar collectors. *Trans. ASME* **2005**, *127*, 60–64.
12. Ji, J.; Pei, G.; Chow, T.T.; Liu, K.; He, H. Experimental study of photovoltaic solar assisted heat pump system. *Sol. Energy* **2008**, *82*, 43–52.
13. Ji, J.; Liu, K.; Chow, T.T.; Pei, G.; He, W.; He, H. Performance analysis of a photovoltaic heat pump. *Appl. Energy* **2008**, *85*, 680–693.
14. Ji, J.; He, H.; Chow, T.; Pei, G.; He, W.; Liu, K. Distributed dynamic modeling and experimental study of PV evaporator in a PV/T solar-assisted heat pump. *Int. J. Heat Mass Transfer* **2009**, *52*, 1365–1373.
15. Xu, G.; Deng, S.; Zhang, X.; Yang, L.; Zhang, Y. Simulation of a photovoltaic/thermal heat pump having a modified collector/evaporator. *Sol. Energy* **2009**, *83*, 1967–1976.
16. Zhao, X.; Zhang, X.; Riffat, S.B.; Su, Y. Theory study of the performance of a novel PV/e roof module for heat pump operation. *Energy Convers. Manag.* **2011**, *52*, 603–614.
17. Tsai H.F.; Tsai, H.L. Implementation and verification of integrated thermal and electrical models for commercial PV modules. *Sol. Energy* **2012**, *86*, 654–665.
18. Million Rooftop PVs Promotion Office. Available online: http://mrpv.org.tw/index.php (accessed on 10 December 2012).
19. Tsai, H.L. Novel photovoltaic/thermal assisted heat pump water heating system. Taiwan Utility Model Patent, Patent No. M432018, 21 June 2012.

20. Peace Software. Available online: http://www.peacesoftware.de/einigewerte/r134a_e.html (accessed on 7 July 2013).
21. Duffie, J.A.; Beckman, W.A. *Solar Engineering of Thermal Process*, 2nd ed.; John Wiley & Sons, Inc.: Hoboken, NJ, USA, 2006; pp. 749–761.